MODIFICAZIONE DI POLIMERI NATURALI AL SERVIZIO DELLE SCIENZE BIOMEDICALI: NANO-CELULOSA, LIGNINA

Prof. Marco Orlandi

Progetto: Dispo09

ATTIVITA' SVOLTA DAL GRUPPO DI RICERCA

- Sintesi di nano-cellulosa cristallina da scarti agro-industriali con metodi "green";
- Modificazione chimica superficiale di nanocellulosa cristallina;
- Primi studi in vitro e in vivo.
- Modificazione selettiva della lignina per ottenere polifenoli e fenoli ad attività antiossidante, antibatterica, batteriostatica

LE BIOMASSE LIGNOCELLULOSICHE

- Il più abbondante materiale grezzo sulla superficie terrestre;
- Composto da cellulosa, emicellulosa e lignina;
- Grandi quantità prodotte come scarto dall'industria agro-alimentare.

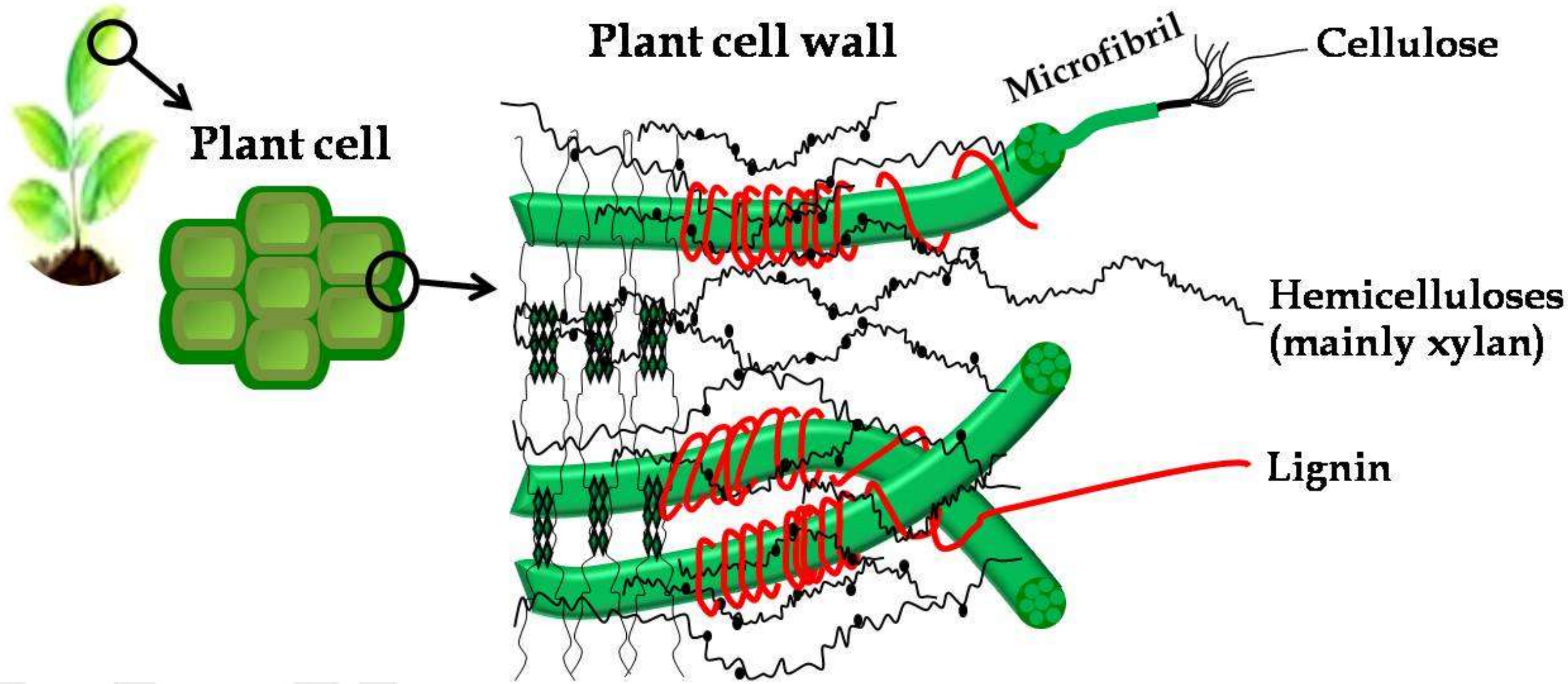

LIGNINA

LIGNIN STRUCTURE: tridimensional, racemic, non-crystalline, hydrophobic polymer that embeds together the lignocellulosic components

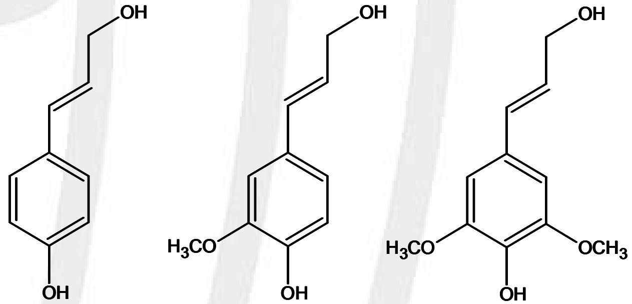

Paracoumaryl alcohol (P-OH) | Coniferyl alcohol (G-OH) | Sinapyl alcohol (S-OH)

Oxidative coupling of mesomeric phenoxy radicals

LIGNIN

Hardwood → **G-OH + S-OH**

Softwood → **G-OH**

Herbaceous → **P-OH + G-OH + S-OH**

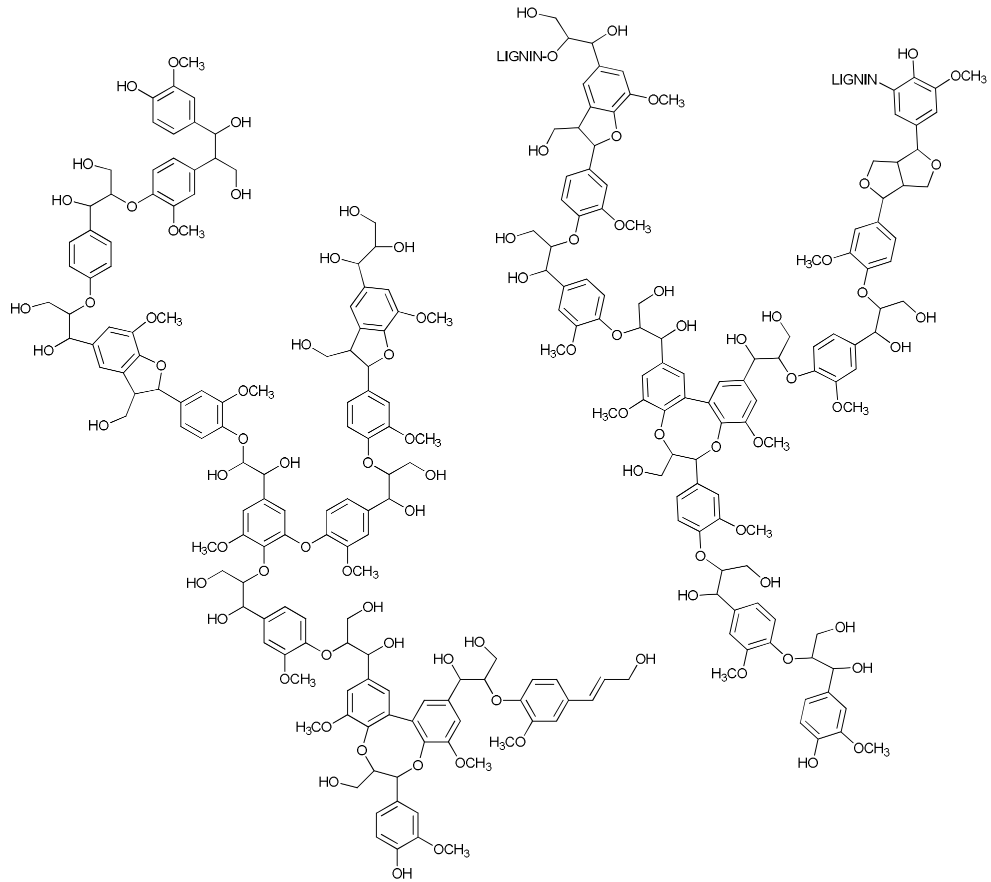

EMICELLULOSA

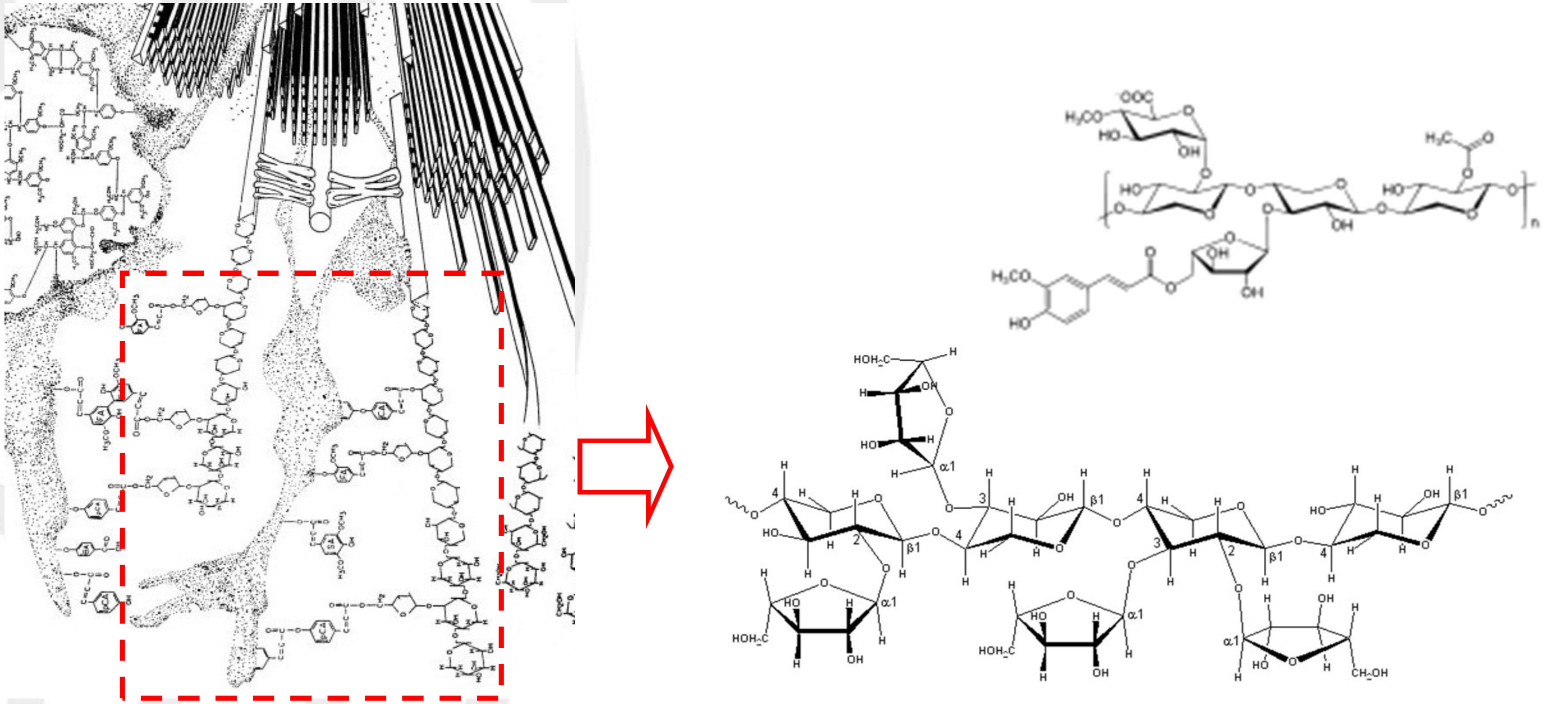

Hemicellulose is composed of carbohydrates based on pentose sugars, mainly xylose and arabinose, as well as hexose sugars, such as glucose and mannose. Mannuronic and galacturonic acid are often present

Shorter, branched chains: 500-3000 sugar units (cellulose: 7000-15000) that cross-link together cellulose fibrils and covalently bind lignin via ester and ether linkages (Lignin-Carbohydrate Complexes, LCC)

Abundant in crop residues, great potential in the production of chemicals

CELLULOSA

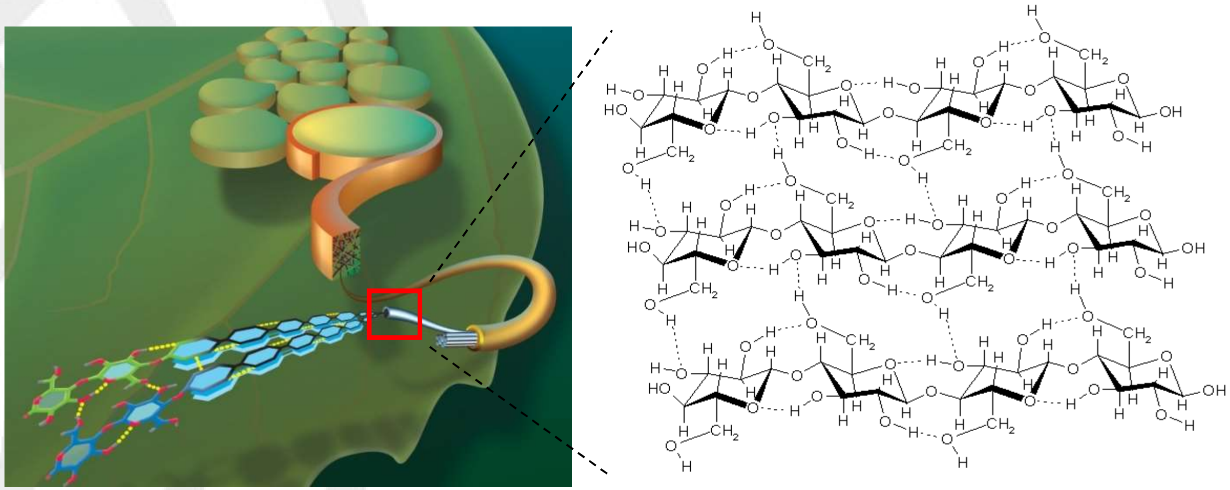

Glucose polymerization (β-1,4 glycosidic linkages)

Chains assembled into sheets (intramolecular + intermolecular H-bonds)

Sheets stacking (Van der Waals)

Spin of the sheets into highly organized fibrils (crystalline and amorphous domains)

Incredibly strong fibers, resistant to the action of enzymes (cellulases) that can crack them back into their simple-sugar components

Mechanical (*mill*)/ chemical (*ionic liquid*) pretreatment required to break cellulose for the production of fuel alternatives

BIOREFINERY PROCESS

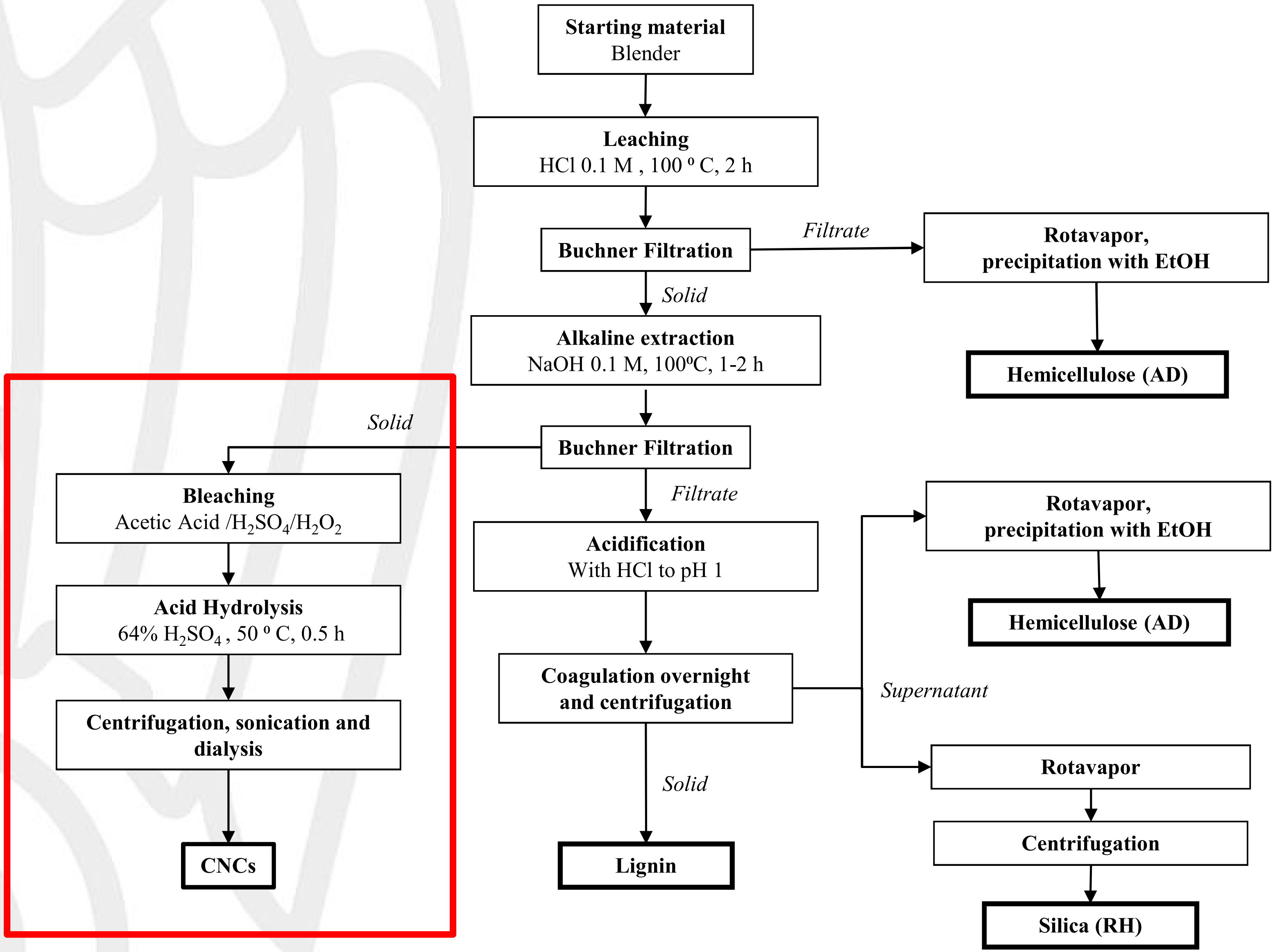

NANO-CELLULOSA
(CNC Cellulose Nano-Crystal)

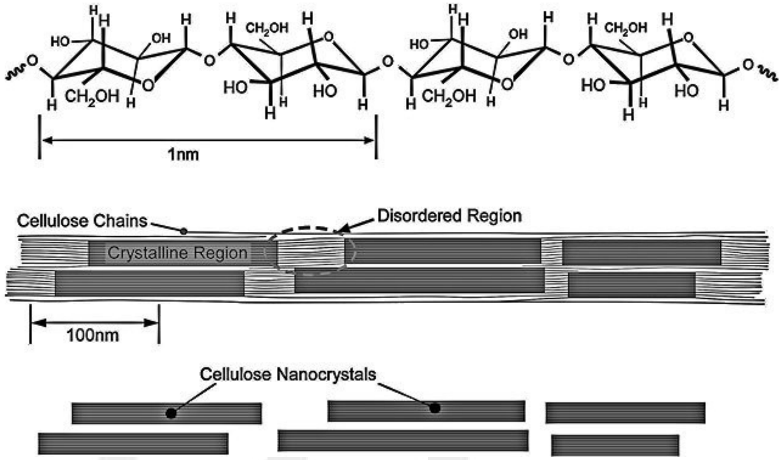

Idrolisi controllata dei domini amorfi e mantenimento di domini cristallini in strutture nanometriche rod-like

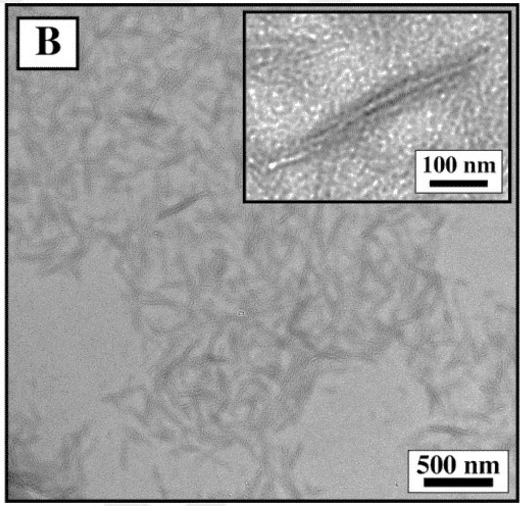

Caratterizzazione TEM

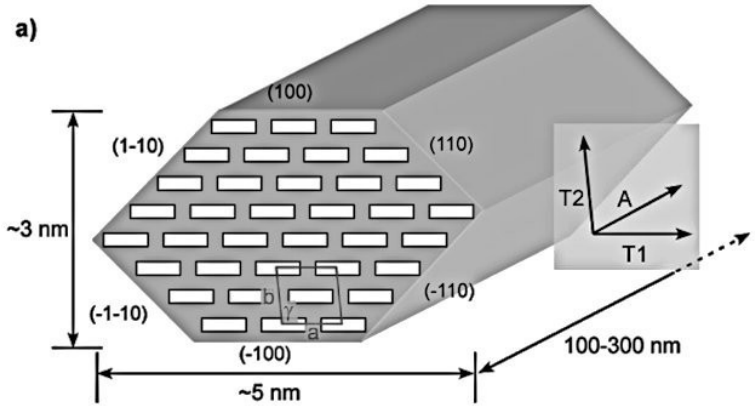

Rappresentazione schematica di CNC

NANO-CELLULOSA

Modifica chimica

Elevata modificabilità superficiale dovuta alla presenza di numerosi siti attivi

Modificazione chimica

Alcol primari

Reducing group

Alcol secondari

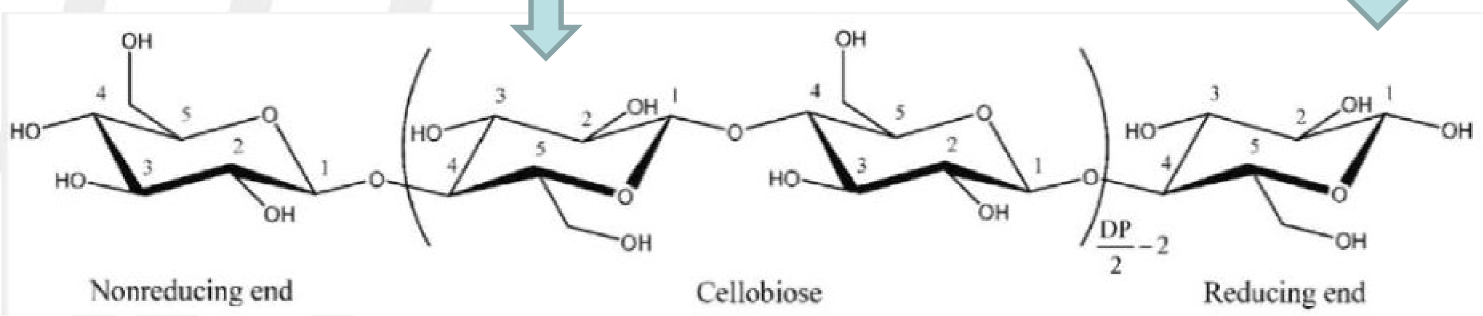

NANO-CELLULOSA

Modifica chimica

Possibilità di reazione sulle funzionalità alcoliche

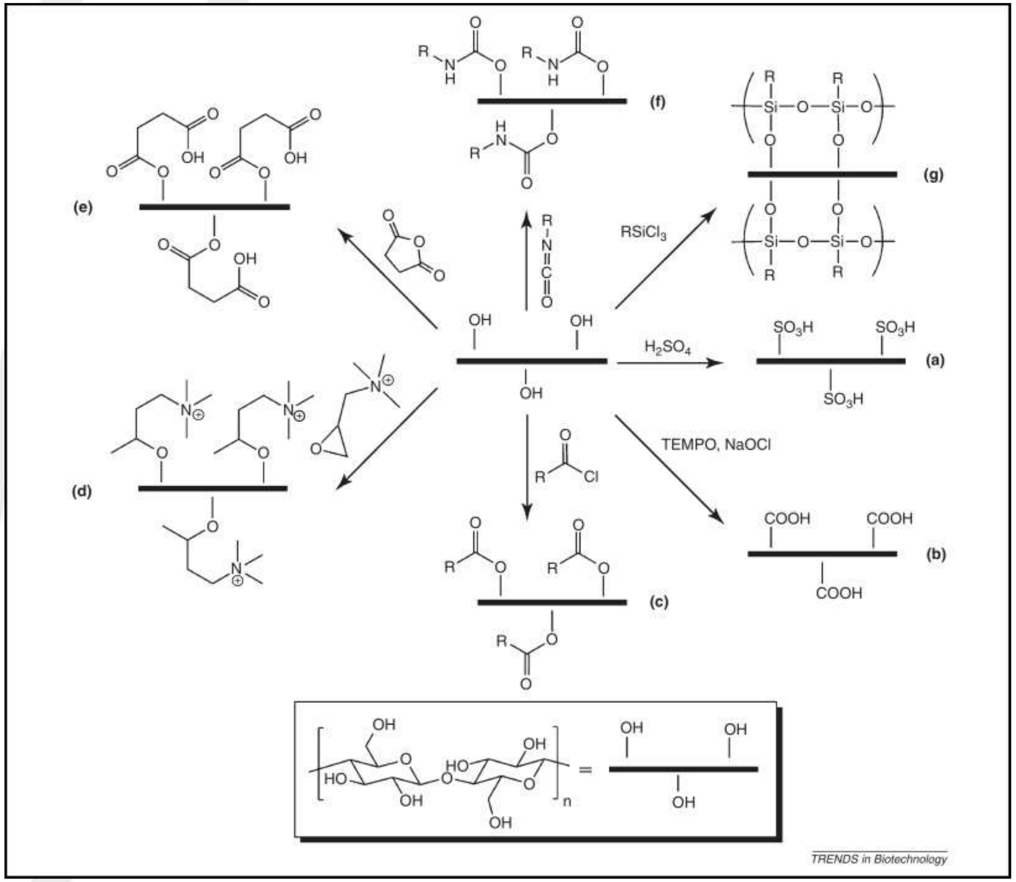

NANO-CELLULOSA

Modifica chimica

Introduzione funzionalità aldeidiche (alto carico) attraverso ossidazione con Periodato di Sodio

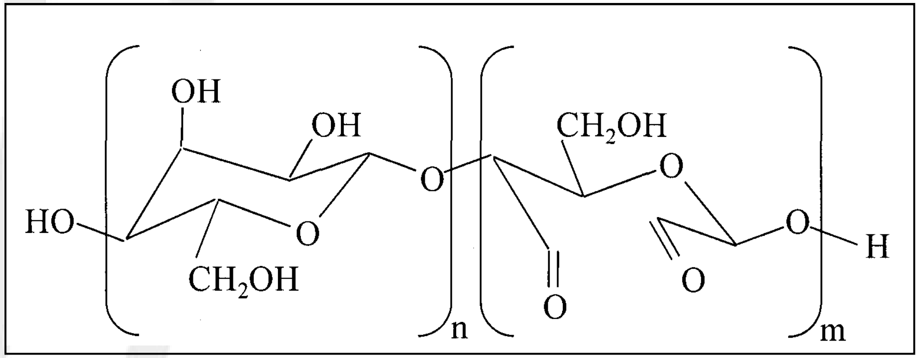

Utilizzo dei reducing end-gruop (basso carico)

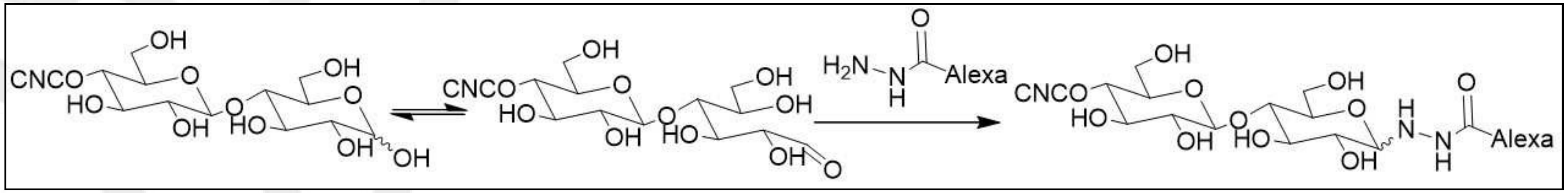

NANO-CELLULOSA

Tropismo sulle ossa

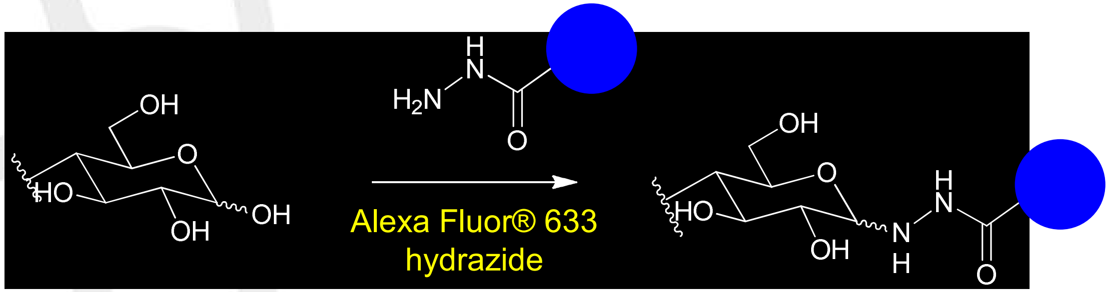

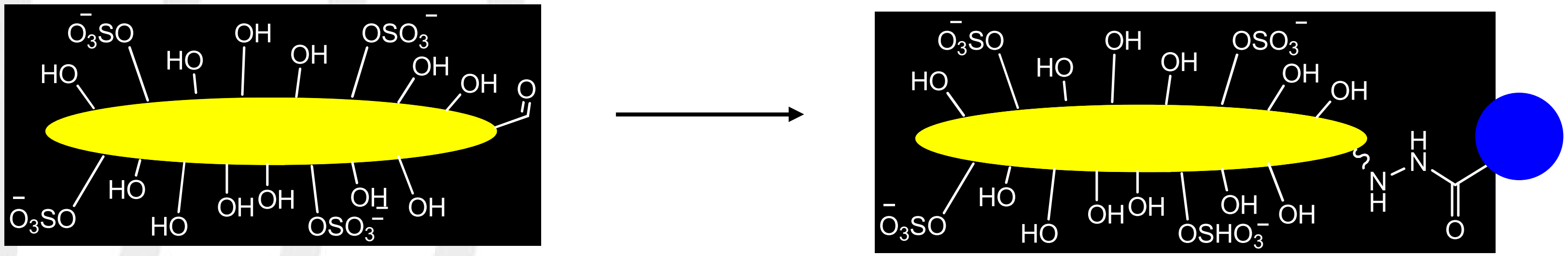

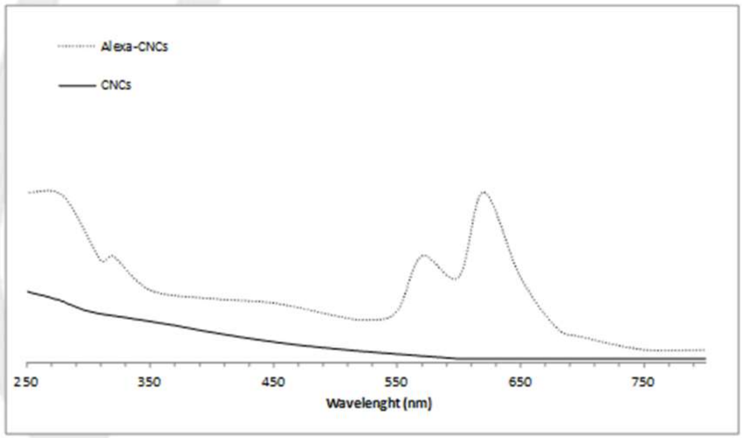

UV analysis of CNCs-Alexa suspension

Isolation, characterization and functionation of cellulose nanocrystals for targeted theranostics in bones.

Laura Colombo[a‡], Luca Zoia[b‡], Martina Bruna Violatto[a], Sara Previdi[a], Laura Talamini[a], Leopoldo Sitia[a], Francesco Nicotra[c], Marco Orlandi[b], Mario Salmona[a], Camilla Recordati[d], Paolo Bigini[a*], Barbara La Ferla[c*]
Biomateril, 2015, Submitted paper.

NANO-CELLULOSA

Tropismo sulle ossa

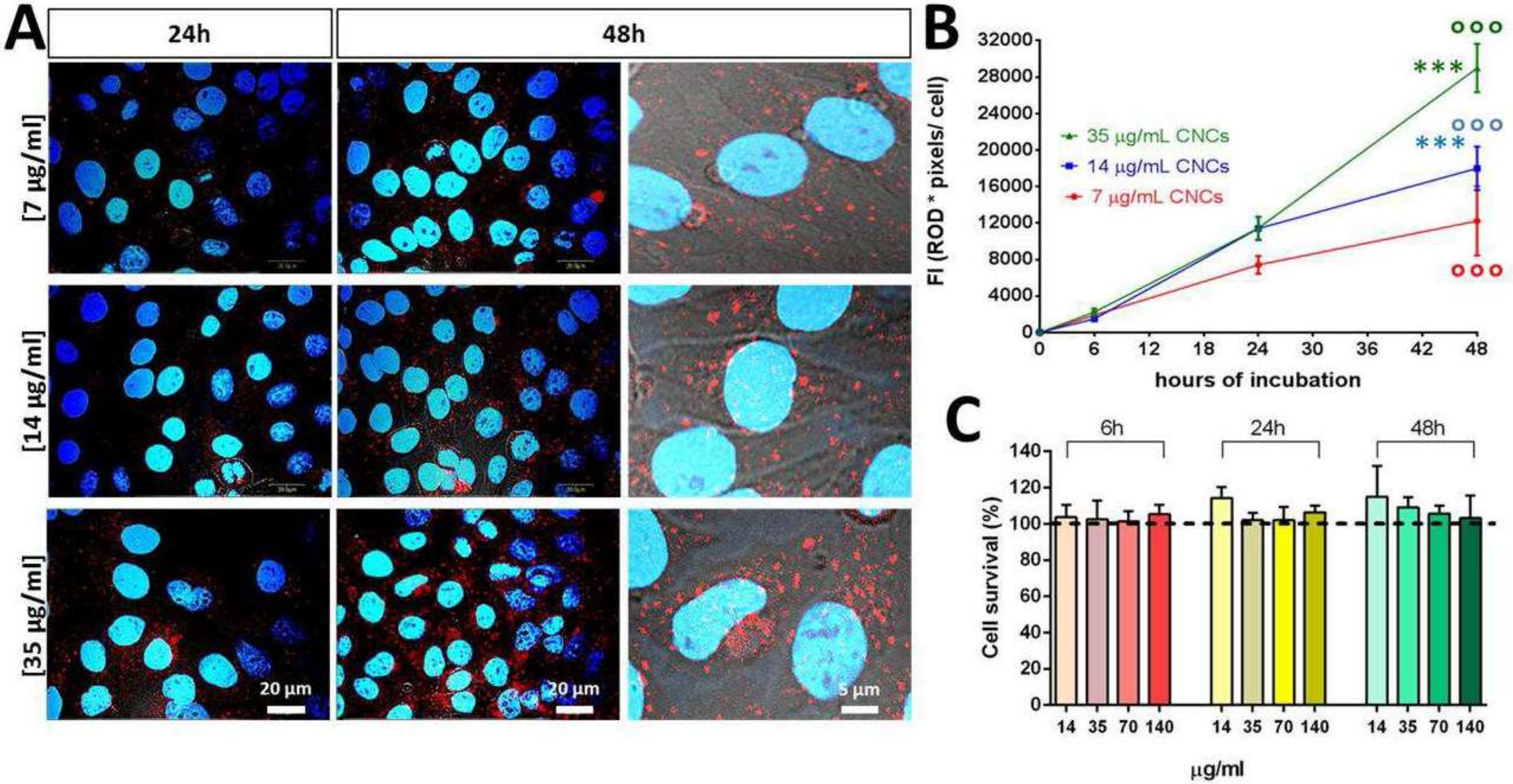

Representative confocal microscopy images showing internalization of different concentrations of CNC-NPs (red signal) in Hela cells (nuclei, blue signal) after 24 and 48 hours of incubation. In the right column, the higher magnification and the merge between fluorescence and nomarski acquisitions reveal that almost all of the red spots are distributed in the cell cytoplasm around the nuclei.

NANO-CELLULOSA

Tropismo sulle ossa

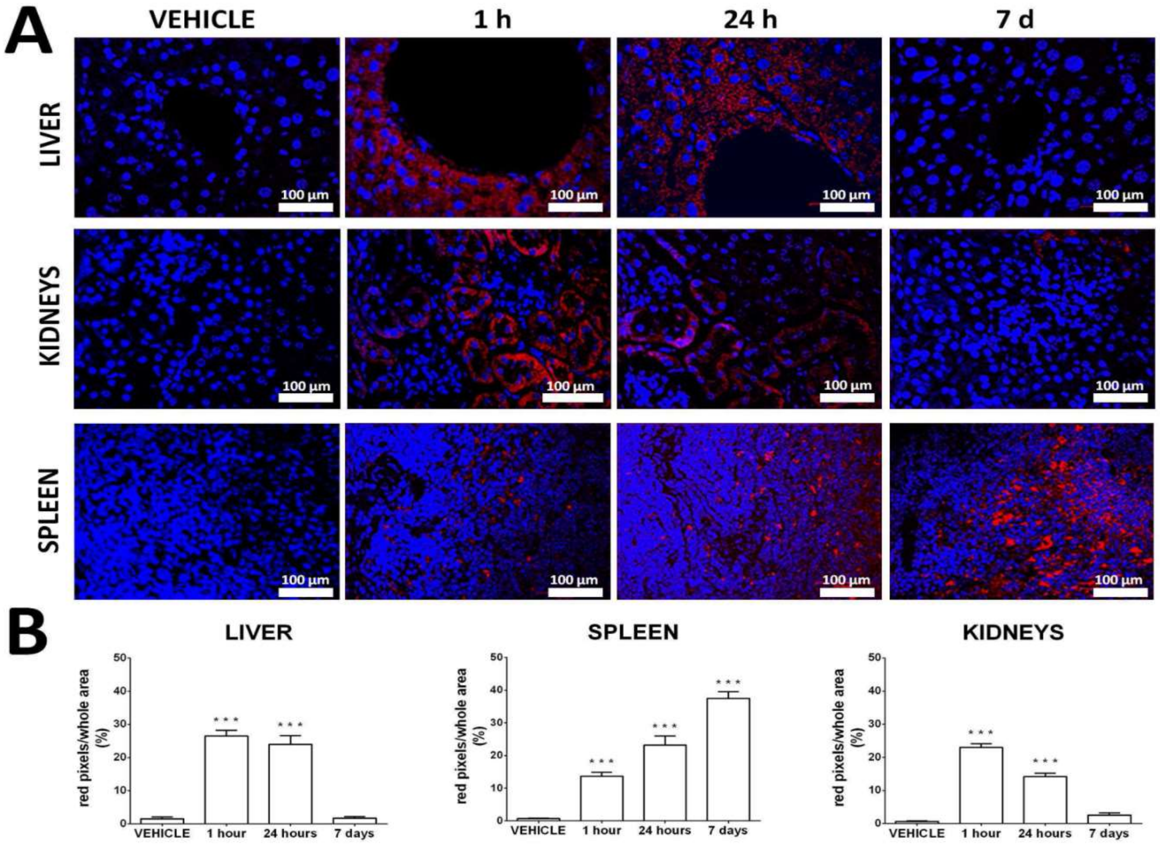

A. Representative microphotographs of liver (upper panels), spleen (E-H) and kidneys (I-L) from NFR mice treated with 120 µl saline solution (first left column) or sacrificed 1- (second column), 24- (third column) or 150 hours (right column) after intravein CNCs injection (a single dose of 120 µl at a concentration of 35 µg/ml). The blue signal is related to the staining of nuclei with the Hoechst 33258 detectable by exciting the sample by the laser with λ = 405 nm. The red staining is associated with Alexa fluorescence, excited by the laser with λ = 635 nm. Scale bars = 100 µm

B. Quantitative measurement of the fluorescence related to Alexa (red) in the three organs depicted above. Data are shown as mean ± S.E. and analyzed by the unpaired Student's t-test. P values ≤ 0.05 was considered as threshold to establish a statically significant difference between vehicle-treated and CNC-treated mice at different time-points (n = 5 for each experimental group).

NANO-CELLULOSA

Tropismo sulle ossa

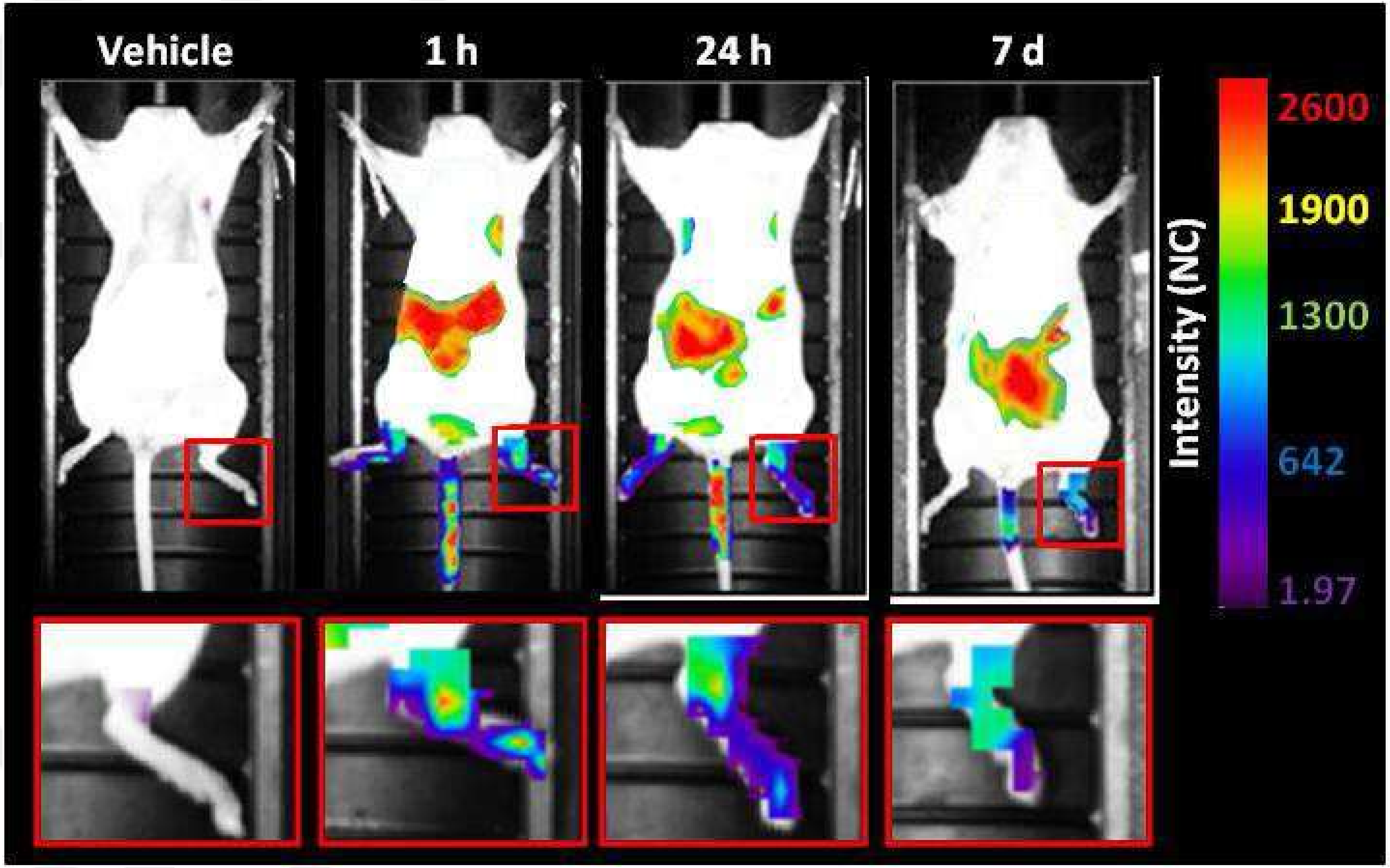

Optical Imaging scans acquired before and 4, 24 and 150 respectively after CNC injection (a single dose of 120 µl at a concentration of 35 µg/ml). Three different regions of interest (ROI) were processed. They were the toraco abdominal area, the tail and the distal hind legs. In the red squares (bottom panels) a higher magnification of the distal hind legs is shown. The fluorescence intensity signal was measured as normalized photon counts (NC) and is shown as a pseudo-color scale bar.

NANO-CELLULOSA

Tropismo sulle ossa

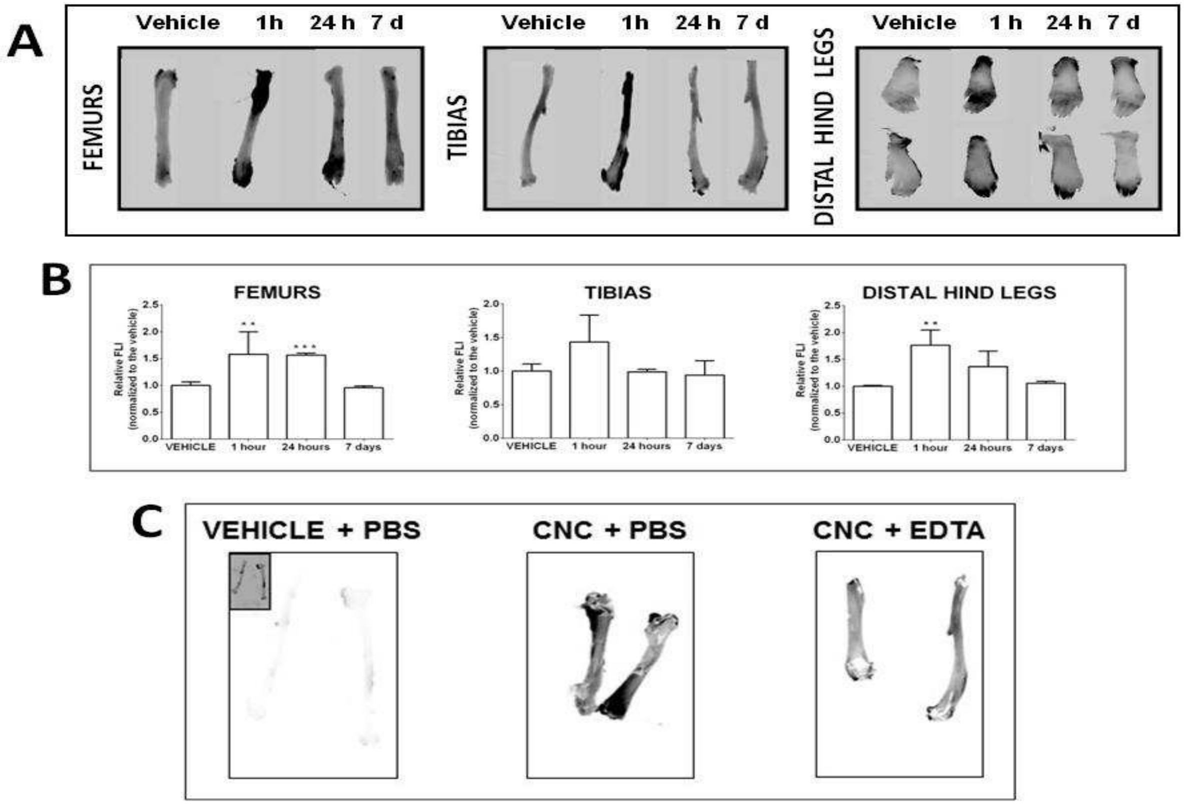

A. Florescence scanning images of femurs, tibias and distal hind legs analyzed with Thyphoon system (λexc laser 633). The fluorescence intensity related to NPs is measured as gray scale and it could range from a minimum (white) to a maximum (black) signal.

B. Quantitative measurement of fluorescence intensity measured in samples normalized to the value of each respective vehicle treated mice. Data are presented as mean ±S.D. and analyzed by one way ANOVA followed by Bonferroni's test. P values ≤ 0.05 was considered as threshold to establish a statically significant difference between vehicle-treated and CNC-treated mice at different time-points (n = 5 for each experimental group).

C. Florescence scanning images of femurs and tibias from bones of control mice in PBS (left- in the top corner a higher contrasted picture of the same sample), incubated for 3 h with CNC (middle) and preincubated in EDTA before CNC incubation (right).

LIGNINA

-Alta reperibilità
-Basso costo
-Struttura oligomerica
-Attività antiossidante

Modificazione chimica

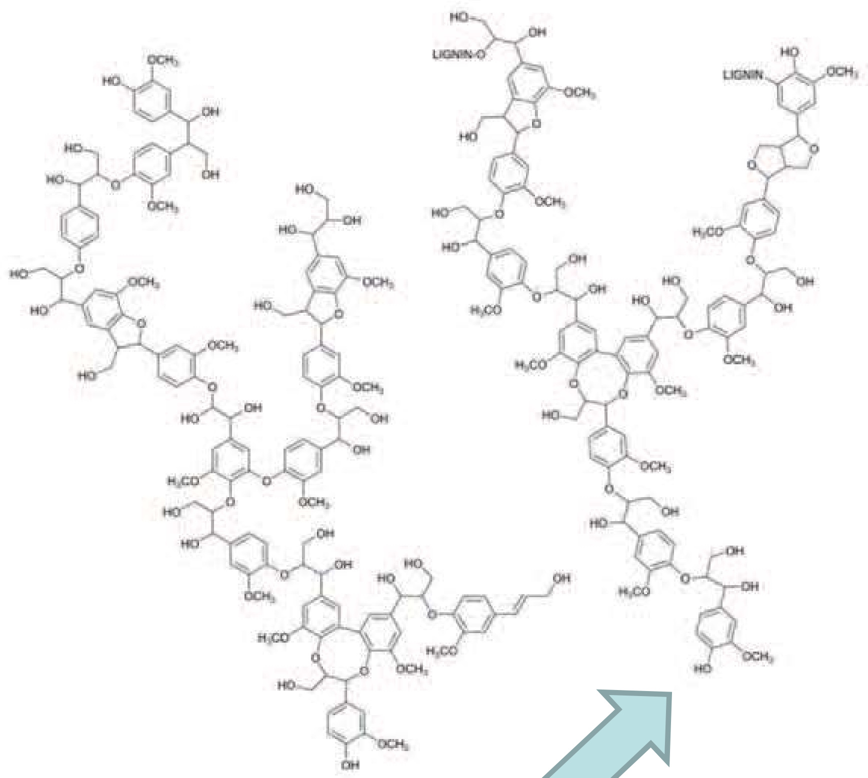

I fenoli sono le unità più facilmente utilizzabili per modifiche chimiche

Però sono anche le unità che conferiscono le proprietà antiossidanti

FENOLI E POLIFENOLI OTTENIBILI DALLA DEPOLIMERIZZAZIONE DELLA LIGNINA

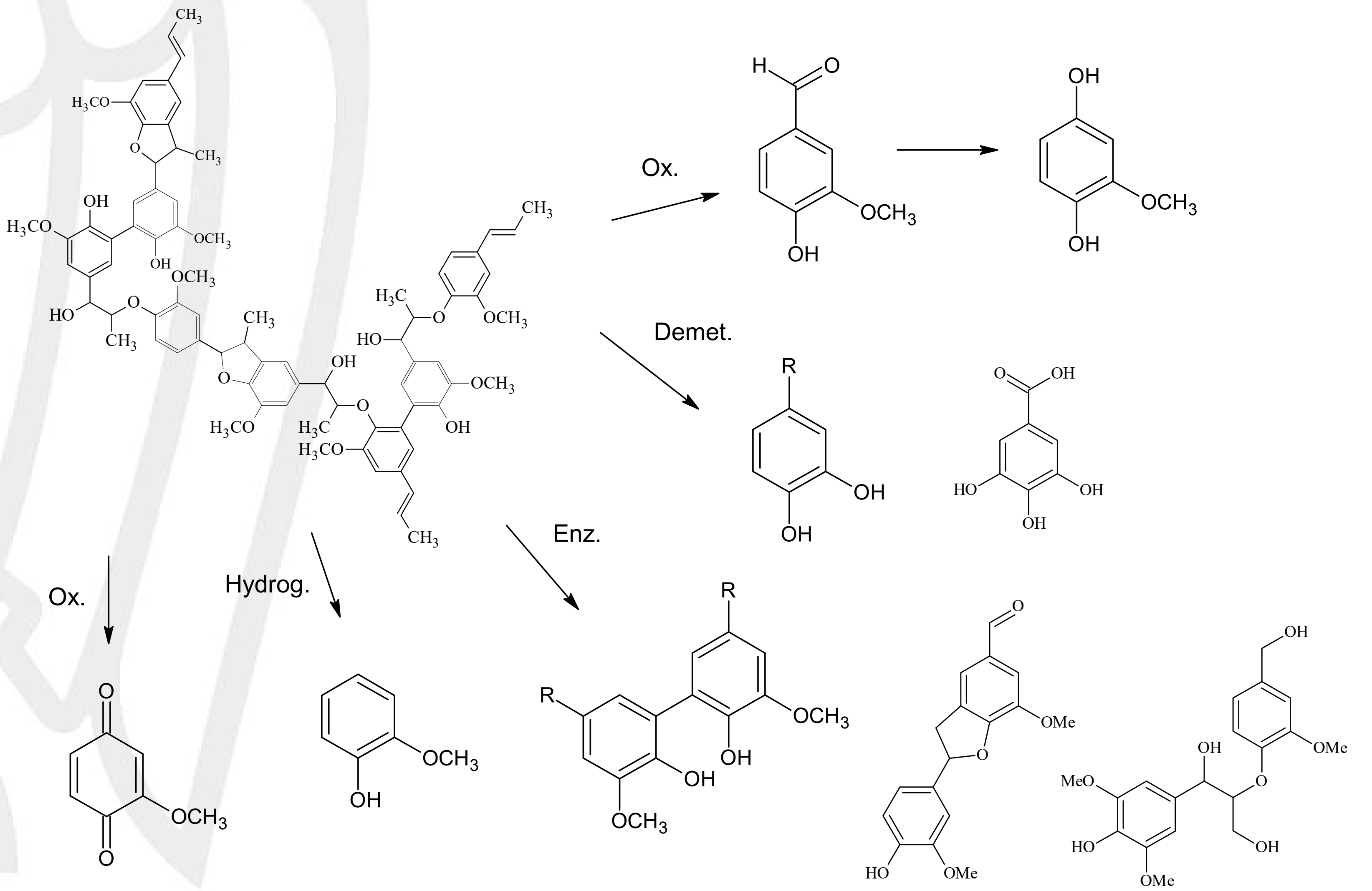

ACIDO IALURONICO

Glicosaminoglucano β1→4 e β1→3, diffuso nei tessuti connettivi

-Elevata Biocompatibilità
-Alto peso molecolare
-Già ampiamente utilizzato
-Attività antiinfiammatoria

Cross-linking tramite modificazione con tioli, metacrilati, ammidi, tiramminine o direttamente con formaldeide o divinilsolfone.

Notevoli applicazioni in:
- cosmesi
- rigenerazione pelle
- scaffold

ACIDO IALURONICO

Modificazione chimica

Gruppi usati per il cross-link (DVS)

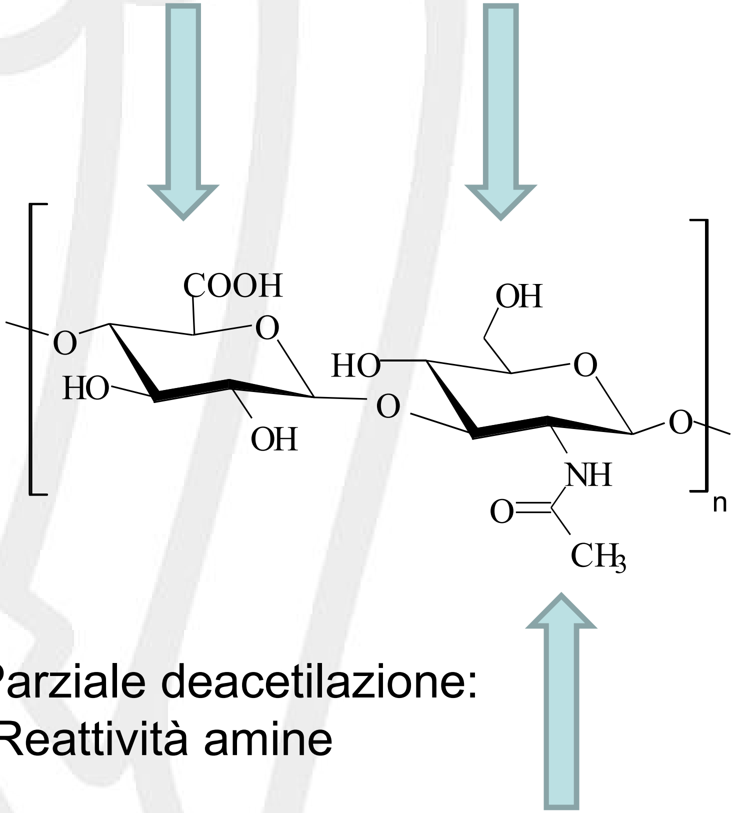

Parziale deacetilazione:
-Reattività amine

-Elevata Biocompatibilità
-Alto peso molecolare
-Già ampiamente utilizzato
-Attività antiinfiammatoria

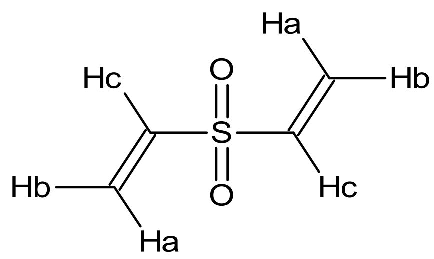

Divinilsulfone (DVS)

Tiramina + HRP H2O2

Conclusioni

- Valorizzazione di scarti a basso valore per la sintesi di nano-devices ad altissimo valore tecnologico e commerciale;

- Assenza di limiti di produzione dovuti alla quasi illimitata disponibilità dei materiali di partenza

- Applicazione di metodi “green” per la sintesi e la modifica